17th World Conference on Earthquake Engineering, 17WCEE
Sendai, Japan - September 13th to 18th 2020

PERIODIC METAFOUNDATIONS FOR THE PROTECTION OF STORAGE TANKS AGAINST VERTICAL GROUND ACCELERATIONS

A. Franchini[(1)], O. S. Bursi[(2)], L. Xiao[(3)], F. Basone [(4)], F. Sun [(5)]

[(1)] PhD Student, Department of Civ., Env. and Geom. Eng., University College London, London, UK, a.franchini.19@ucl.ac.uk
[(2)] Full Professor, Department of Civ., Env. and Mech. Engineering, University of Trento, Trento, ITALY, oreste.bursi@unitn.it
[(3)] PhD Student, College of Civil Engineering, Tongji University, Shanghai, CHINA, 1410213@tongji.edu.cn
[(4)] PhD Eng. and Architecture Faculty, University of Enna "Kore", Enna, ITALY, francescobasone@gmail.com
[(4)] Full Professor, College of Civil Engineering, Tongji University, Shanghai, CHINA, ffsun@tongji.edu.cn

Abstract

An innovative way to protect storage tanks against earthquake consists in implementing finite lattice locally resonant metafoundations. A remarkable property of these systems is their capacity of protecting the structure against the vertical component of ground accelerations, which entails additional pressure on the tank walls. Vertical seismic isolation cannot be achieved with conventional rubber bearings, that are very stiff in the vertical direction. Therefore, we consider a metafoundation formed by an external columns-slab frame and concrete resonators (connected by means of wire ropes) and study three feasible configurations for vertical isolation purposes. Resonators properties are optimized and the performance of the proposed systems is assessed in time domain. Moreover, we validate the linearly elastic symmetric behaviour assumption for wire ropes and investigate the influence of soil structure interaction (SSI) on the attenuation of hydrodynamic pressure. Results show that it is possible to design metafoundations for vertical isolation and that better performances can be achieved with a staggered-columns frame. Eventually, it can be observed that SSI modifies the attenuation capacity of the considered systems: this fact highlights the necessity of developing a more detailed optimization procedure, able to consider the effects interaction between soil, foundation and superstructure.

Keywords: seismic risk mitigation; industrial facilities; slender tank; broad tank; soil-structure interaction; finite-lattice metamaterials; attenuation zones.

1. Introduction

Metamaterials show particular properties, not found in nature, when interacting with a propagating wave. In particular, they can be designed such as to forbid or reduce elastic wave propagation in a selected range of frequencies. In this respect, Liu et al. [1] proposed three-component composites consisting of hard spheres coated with a soft cladding and arranged in a stiff host medium. Thanks to local resonance of the spheres, this system is able to realize band gaps with lattice constants of several orders of magnitude smaller than mechanical wavelengths travelling across them. These properties could be applied for seismic isolation purposes; a possible way to do so is to design locally resonant foundations for structures, which are referred to as 'metafoundations' hereinafter. Jia and Shi [2] proposed a 2D metafoundation formed of steel cylinders coated by rubber and embedded in a concrete matrix, which was implemented for the seismic protection of a six-stories building. Significant contributions to further development of this system can be found in the works of Shi and Huang [3], Cheng and Shi [4], Yan et al. [5], Yan et al. [6], Huang et al. [7], Cheng and Shi [8], Casablanca et al. [9], Witarto et al. [10], Liu et al. [11]. Moreover, La Salandra et al. [12], Wenzel et al. [13] and Basone et al. [14] proposed the use of metafoundation to protect liquid storage tanks against horizontal ground shaking. Within this framework, Sun et al. [15] investigated the effects of horizontal soil-structure interaction (SSI). Nevertheless, the literature presents a lack in feasible solutions to isolate storage tanks against the effect of vertical components of earthquakes.

In this paper, we study feasible metafoundation configurations, which are able to protect a selected storage tank from vertical ground shaking. More specifically, we study three feasible configurations for the foundation frame, distinguished by the number of layers and the arrangement of columns, and we assess their performances through time history analyses. In addition, we validate the linear symmetric behaviour assumption for wire ropes and investigate the effects of vertical SSI on metafoundation performance.

Table 1 – Material properties.

Material	Density [kg/m^3]	Elastic modulus [N/mm^2]	Bulk modulus [N/mm^2]	Poisson ratio	Strength [N/mm^2]
Steel	7860	210000	-	0.28	275
Liquid	1000	-	2200	-	-
Concrete C40/50	2500	30000	-	0.20	40
Reinforcement	7850	210000	-	0.28	550

2. Storage tank and novel metafoundation

In this research, we aimed at the protection of a slender, cylindrical storage tank containing liquid, which is located in the refinery of Priolo Gargallo. The tank's geometric characteristics are as follows: radius R=4.00m, liquid height H=12.00m, wall thickness h=6.00mm. Table 1 lists the material properties. In this type of structure, the vertical component of ground acceleration induces additional horizontal hydrodynamic pressure p_v which increases the hoop stress in the wall; such a pressure, can be calculated by means of the following equation [16]:

$$p_v(t) = p_s(t) + p_{vb}(t) + p_{vi}(t) \quad (1)$$

In detail, t is the time; p_{vs} is the long-period component deriving from the convective fluid motion; p_{vi} is the impulsive fluid pressure component which varies in synchronism with the vertical ground acceleration; p_{vb} the short-period component, derives from the tank walls radial, axisymmetric vibration. Such a vibration is called

breathing mode and an example is presented in Fig.1a from [17]. The calculation of the induced pressure can be conducted by means of a low-fidelity model, which is described in Subsection 3.1.

Basone et al. [14] introduced a novel metafoundation for the reduction of horizontal ground motion - induced vibrations in fuel storage tanks. The isometric view of the system is presented in Fig.1b. Its horizontal section consists of nine square shaped unit cells of 3m side, composed by steel hollow columns and 200 mm thick concrete slabs. A single-layered (L1) and a two-layered (L2) configurations are considered; the total height of the frame is 3m in both cases. As highlighted in Fig.1c, in each unit cell, a concrete parallelepiped called resonator is connected to the upper and to the lower slab by means of special devices called wire ropes. They consist of a stainless steel cable that is spirally wrapped and blocked by two steel bars as shown in Fig.2c [18, 19]. This configuration entails high flexibility in both the horizontal -roll and shear- and vertical -tension-compression- directions. In addition, vibrational energy damped out by means of friction between wires forming the cable. Wire ropes show a hysteretic and non-linear behaviour, which was characterized in detail in the literature. Nevertheless, for small relative displacements a linearly elastic symmetric behaviour can be assumed. Hereinafter, we focus on the attenuation of the vertical shaking-induced wall pressure p_v, and therefore we only consider the Tension-Compression behaviour of wire ropes, see Fig. 2d.

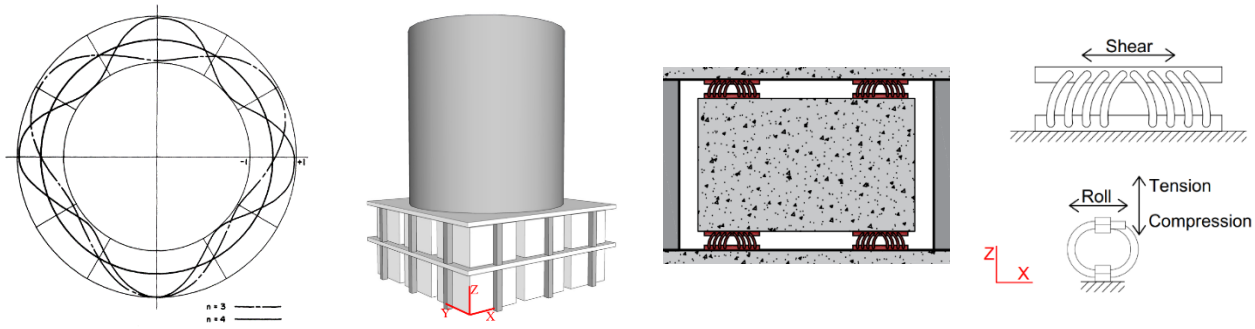

(a) (b) (c) (d)

Fig. 1 – (a) 3rd and 4th breathing vibrational mode of a cylindrical shell containing liquid [17]; (b) isometric view of the coupled foundation-tank system proposed in [14]; (c) connection of a resonator to the slabs; (d) geometrical and kinematic characteristics of a wire rope.

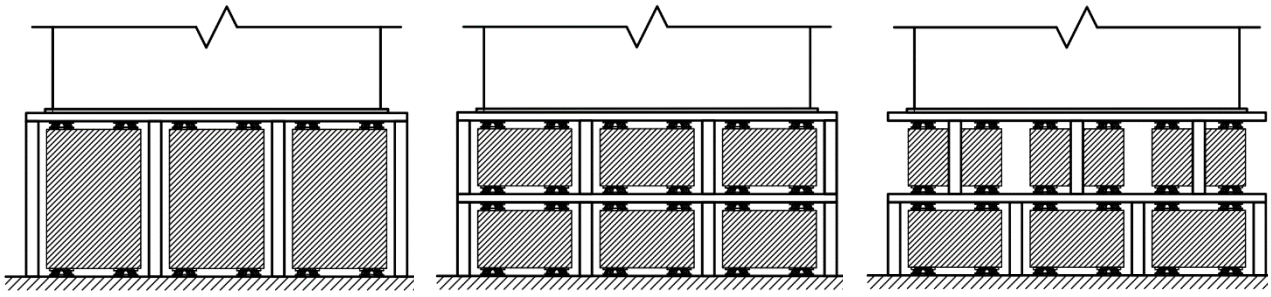

(a) (b) (c)

Fig. 2 – Proposed metafoundation configurations for vertical seismic attenuation: (a) single-layered L1; (b) two-layered aligned columns L2a; (c) two-layered staggered columns.

As well-known from base isolation theory, and also according to [14], the seismic response of the superstructure can be reduced by means of a low-stiffness connection between the tank and the soil. In the considered metafoundation, this requires the reduction of the external frame stiffness, which depends on the axial stiffness of columns. A possible way to achieve this goal is to take advantage of slabs flexural stiffness,

which is lower than the columns axial stiffness. To this end, columns at the first level are located at the vertex of the square projection of every unit cell, while those at the second level are staggered with respect to the previous ones. As a result, we distinguish two types of two-layered metafoundation: L2a, with aligned columns, and L2s which presents a staggered-columns configuration. Thus, in the following part of the paper, we investigate the attenuation capacity of the three configurations L1, L2a and L2s, distinguished by the number of layers and the arrangement of columns. They are depicted in Fig.2, while their properties are summarized in Table 2.

Table 2 – Geometrical properties of the proposed metfoundation configurations.

Foundation	**L1**	**L2a**	**L2s**
Layers	1	2	2
Columns arrangement	\	Aligned	Staggered
Height of one layer [m]	3	1.5	1.5
Slab thickness [mm]	200	200	230
Column side [mm]	250	200	200
Column thickness [mm]	30	30	35
Columns at layer 1	24	24	16
Columns at layer 2	0	24	24

A main concern for the staggered-columns frame is the risk of punching shear at the point in which the columns at the second level connect to the first-level slab. Therefore, the slab thickness was increased to 230mm and punching reinforcement was carefully designed. Fig.3a shows the FE model we built in the commercial software ETABS (Computers and Structures, Inc.) and highlights possible locations where punching shear

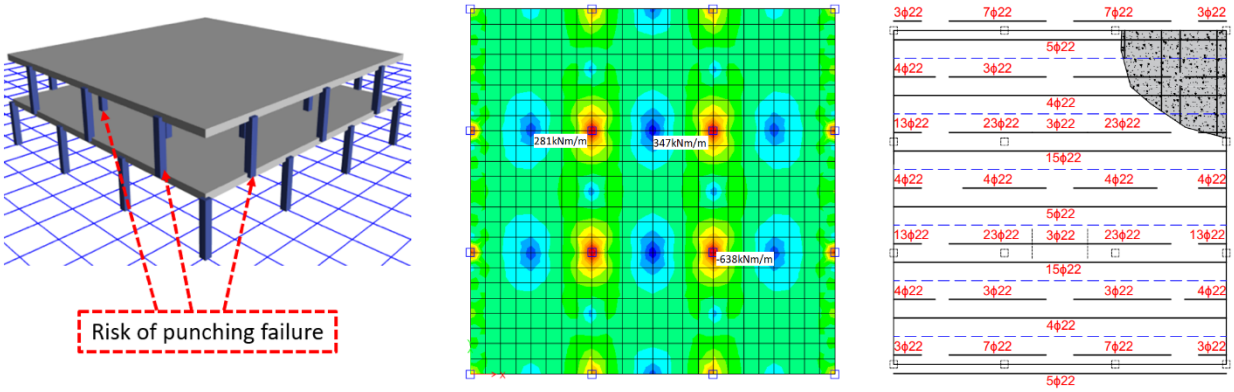

(a) (b) (c)

Fig. 3 – (a) FE model of the metafoundation in the commercial software ETABS; (b) moments per unit length in the first-level slab; (c) required reinforcement.

failure may happen. Columns and slabs were modelled by means of frame elements and thin-shell elements, respectively. As suggested in [20], the cracking of concrete under seismic loading was taken into account by reducing its elastic modulus by 50%. The load of the tank was taken into account as a shell load of 122kN/m2, whereas every resonator was represented by means of four concentrated loads with a magnitude equal to one fourth of the resonator weight. The response spectrum method was used to model the seismic action in the vertical direction, considering a return period T_R=2475y and the parameters prescribed by the Italian standards

[20]. From this model, we obtained bending moments per unit length, as shown in Fig.3b for the first-level slab; accordingly, we designed the required reinforcement in the two directions, as presented in Fig. 3c.

3. Analytical models and optimization

3.1 Tank model

In order to calculate the pressure p_v, defined in Eq. (1), Veletsos and Tang [21] proposed the low-fidelity mass-spring model depicted in Fig. 4a. A portion of the liquid mass m_l, corresponding to the impulsive mode and denoted as m_{vi}, is rigidly linked to the tank base; the remaining mass, corresponding to the breathing mode and denoted as mb, is flexibly connected thorough a spring k_b. The contribution of the convective fluid motion p_{vs} is neglected. Therefore, $m_l=m_{vi}+m_b$. The breathing mass can be calculated as $m_b=m_l\cdot\alpha_m$, where α_m is a nondimensional factor. The natural frequency of the breathing mode is obtained as $\omega_b=\omega_0\cdot\alpha_\omega$, in which is another nondimensional factor. Both α_m and α_ω are tabulated as a function of the tank slenderness (ratio H=R of liquid height to tank radius) and can be found in [21]. ω_0 represents the natural frequency of the breathing mode for a ring with the same cross section as the tank wall and can be obtained as:

$$\omega_0 = \frac{1}{R}\sqrt{\frac{E_t}{\rho_t}} \tag{2}$$

E_t and ρ_t are the tank material elastic modulus and density, respectively. The breathing stiffness can be calculated as $k_b=m_b\cdot\omega_b$, while m_{vi} is obtained by subtracting the value of the breathing mass to the value of the total liquid mass. The mass of the wall of the tank m_t is assumed as rigidly attached to m_{vi}, whereas the damping ratio of the breathing mode is taken as $\xi_b=0.005$. The resulting properties of the tank model are shown

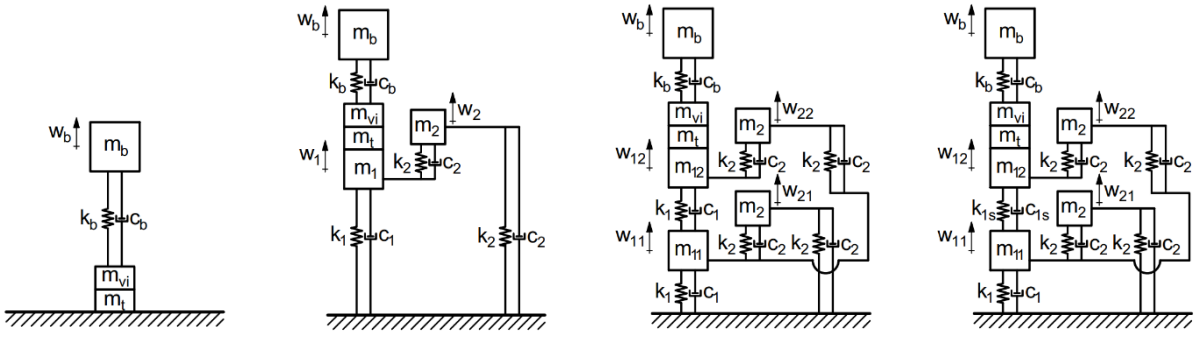

(a) (b) (c) (d)

Fig. 4 – Implemented analytical models: (a) uncontrolled tank; (b) L1; (c) L2a; (d) L2s.

in the left side of Table 3. Let $\ddot{z}_{vi}$ and $\ddot{z}_b$ be the accelerations of the vertical impulsive mass and of the breathing mass, respectively. According to EC-8 Part 4 [22], the terms p_{vi} and p_{vb} in Eq. (1) read:

$$p_{vi}(t) = \rho_l H_l \ddot{z}_{vi}(t) \tag{3}$$

$$p_{vb}(t) = 0.815[1.078 + 0.274\log\left(\frac{H_l}{R}\right)]\rho_l H\ddot{z}_b(t) \tag{4}$$

In the case of uncontrolled tank, i.e. when the tank lays directly on the soil without metafoundation, the acceleration of the vertical impulsive mass equals the acceleration of the ground.

3.2 Metafoundation model

The dynamic modelling of the foundation is carried out by condensing both masses and stiffnesses of resonators, slabs and columns at each layer to one stack of unit cells. In the case of the staggered-columns

configuration L2s, the vertical stiffness depends on the in-series combination of columns axial stiffness and slabs flexural stiffness, which is determined by applying Force Method to the previously described FE model. Hereinafter, the properties of the condensed metafoundation models are named as follows: m11and m12 are the condensed masses (columns and slab) at the first and second level, respectively; k1 is the condensed stiffness of the columns at the first level; k_{1s} is the condensed stiffness of the in-series column-slab elements at the second level for the staggered configuration; in the case of L2a, $k_{1s}=k_1$; m2 and k2 are the condensed masses and stiffnesses of the resonators; c_2 is the dashpot of the resonators, obtained as $c2=2\xi_2(k_2m_2)^{(1/2)}$, with ξ_2 to be optimized. The properties of metafoundation models are listed in the right-side of Table 3, where it is worth to notice that the staggered stiffnesses are about one order of magnitude smaller than the aligned ones.

Table 3 – Dynamic models properties.

Tank model				**Metafoundation model**			
Mass of the tank	mt	18.94	ton	m11 [ton]	57.48	47.29	45.78
Mass of the liquid	ml	603.19	ton	m12 [ton]	\	47.29	48.42
Breathing mass	mb	468.68	ton	m2 [ton]	267.91	133.95	133.95
Vertical impulsive mass	mvi	134.51	ton	k1 [kN/mm]	144000	57600	44800
Natural frequency of the first breathing mode	ωb	42.28	rad/s	k1s [kN/mm]	\	57600	2974
Breathing stiffness	kb	837.91	kN/mm	k2 and c2	To be optimized	To be optimized	To be optimized

3.3 Coupled system and equations of motion

The coupled tank-metafoundation systems are obtained by rigidly attaching the impulsive mass of the tank to the superior slab of the metafoundation, as shown in Fig. 4b-d. Therefore, the equations of motion (EOM) for systems subjected to a vertical ground motion $\ddot{z}_g$ read:

$$\mathbf{M}\ddot{\mathbf{w}}(t) + \mathbf{C}\dot{\mathbf{w}}(t) + \mathbf{K}\mathbf{w}(t) = -\mathbf{M}\mathbf{I}\ddot{z}_g(t) \tag{5}$$

where **M**, **C** and **K** are system mass matrix, damping matrix and stiffness matrix respectively; **w**(t) is the vector of displacement relative to the ground motion; **I** is the unitary vector. As described in Subsection 3.1, the uncontrolled tank is modelled as a SDoF system, and therefore the EOM to calculate the acceleration response of the breathing mass is:

$$m_b\ddot{w}_b(t) + c_b\dot{w}_b(t) + k_b w_b(t) = -m_b\ddot{z}_g(t) \tag{6}$$

3.4 Metafoundation optimization

In the assumption of dealing with a stationary dynamic process with power spectral density (PSD) $S_g(\omega)$, the acceleration response PSD at the i-th DoF of a system can be calculated as

$$S_i(\omega) = \left|\ddot{Z}_i(\omega)\right|^2 S_g(\omega) \tag{7}$$

where $\ddot{Z}_i(\omega)$ is the absolute vertical acceleration transfer function of the i-th DoF. In a slender storage tank, as the one considered in this research, the breathing mass gives the highest contribution to the base pressure.

Therefore, we refer to the breathing mass absolute acceleration $\ddot{Z}_b(\omega)$ for the optimization procedure. By assuming a zero-mean process, the integral over frequency of the PSD represents the average total power, or variance of the absolute acceleration response:

$$\sigma^2_{\ddot{Z}_b} = \int_0^\infty S_b(\omega)\, d\omega = \int_0^\infty \left|\ddot{Z}_i(\omega)\right|^2 S_g(\omega)\, d\omega \tag{8}$$

As for the PSD of the ground, we implemented the Kanai-Tajimi model, which simulates a site-specific PSD as stationary Gaussian-filtered white noise random process with zero mean and spectral intensity S0:

$$S_g(\omega) = S_0 \frac{\omega_g^4 + 4\zeta_g^2\omega_g^2\omega^2}{\left(\omega_g^2 - \omega^2\right)^2 + 4\zeta_g^2\omega_g^2\omega^2} \tag{9}$$

Table 4 – Optimal parameters for the resonators.

Type of soil	Parameter	L1	L2a	L2s
Type A, dense	$\omega_{2,opt}$	41.44	41.24	37.82
	$\xi_{2,opt}$	0.01	0.01	0.02
	min{PI}	0.968	0.739	0.344
Type B, medium	ω2,opt	41.44	41.24	37.79
	ξ2,opt	0.01	0.01	0.02
	min{PI}	0.972	0.759	0.414
Type C, loose	ω2,opt	41.44	41.24	37.79
	ξ2,opt	0.01	0.01	0.02
	min{PI}	0.972	0.761	0.426

We considered three types of soil according to the Italian standards [20], namely soil Type A, Type B and Type C, for which Kanai-Tajimi parameters are assumed as follows: for Type A, $S_0 = 0.013\text{m}^3/\text{s}^2$ and $\omega_g = 38.80\text{rad/s}$; for Type B, $S_0 = 0.018\text{m}^3/\text{s}^2$ and $\omega_g = 29.10\text{rad/s}$; for Type C, $S_0 = 0.020\text{m}^3/\text{s}^2$ and $\omega_g = 26.20\text{rad/s}$. Eventually, we defined a performance index as the ratio of the variance of breathing mass breathing mass acceleration in a controlled tank to the uncontrolled one, i.e. $\text{PI} = \sigma^2_{\ddot{Z}_b,\text{CON}}/\sigma^2_{\ddot{Z}_b,\text{UNCON}}$. The optimization problem consists in finding the combination $\{\xi_2,\ \omega_2\}$ which minimizes PI; in this respect, results are given in Table 4. Wire ropes WR36-400-08, WR28-400-08 and WR36-600-08 are accordingly chosen from a catalogue [23].

4. Time history analysis

4.1 Accelerograms selection

The tank we study is located in the refinery of Priolo Gargallo, in the south of Italy, where the soil is classified as Type B. In order to model the seismic activity at the construction side, we selected a set of seven natural accelerograms with 10% probability of exceedance in 50 years; they are listed in Table 5. These seismic records were selected so that their mean spectrum fits in a least-square sense the uniform hazard spectrum (UHS) at the construction site. It is well-known that the UHS is overly conservative, since it is obtained as the envelope

of spectral amplitudes of accelerograms at all periods that are exceeded with a certain probability for a certain number of years. Because of this, it is not deemed necessary to use a conditional mean spectrum that matches the UHS level only at the fundamental period of a system; as a consequence, the same set of accelerograms can be used to study the response of all the considered foundation-tank coupled systems.

Table 5 – Selected natural accelerograms.

Acronym	Event	Country	Date	Station	Magnitude Mw	PGA [m/s^2]
Acc1	South Iceland (aftershock)	ISLANDA	21/06/2000	ST2484	6.4	3.71
Acc2	South Iceland	ISLANDA	17/06/2000	ST2482	6.5	1.78
Acc3	Ano Liosia	GREECE	07/09/1999	ST1259	6.0	1.93
Acc4	L'Aquila Mainshock	ITALY	06/04/2009	AQA	6.3	4.35
Acc5	L'Aquila Mainshock	ITALY	06/04/2009	AQG	6.3	2.35
Acc6	L'Aquila Mainshock	ITALY	06/04/2009	AQK	6.3	3.55
Acc7	L'Aquila Mainshock	ITALY	06/04/2009	AQV	6.3	4.87

4.2 Mitigation effect and wire ropes behaviour

In order to evaluate the efficacy of the proposed metafoundation, we study the time history of the hydrodynamic base pressure. To this end, EOM from Eq. (5) are solved by means of Newmark Method and DoF's accelerations are calculated; then, Eqs. (1,3-4) are implemented to obtain the history of base pressure. As an example, Fig. 5a shows the base pressure induced by Acc5. In this figure, it is clearly shown that the metafoundation configurations we proposed can efficiently reduce the superstructure response; moreover, a better performance is achieved by reducing the external frame stiffness. In this respect, the highest attenuation is obtained by implementing the staggered columns metafoundation L2s.

For a given accelerogram $\ddot{z}_{g,j}(t)$, the root mean square (RMS) of the base pressure can be calculated as:

$$p_{v,j}^{RMS} = \sqrt{\frac{1}{n_i}\sum_{i=1}^{n_i}\left|p_{v,j}(t_i)\right|^2} \tag{10}$$

Where t_i are the n_i discrete points in time domain at which the accelerogram was recorded. Based on Eq. (10), we defined an index α as ratio of the controlled RMS to the uncontrolled RMS:

$$\alpha_j = \frac{p_{v,con,j}^{RMS}}{p_{v,uncon,j}^{RMS}} \tag{11}$$

When the index is less than 1, a superstructure response attenuation is pointed out. Therefore, α can be taken as an indication of the metafoundation performance against a specific accelerogram. The index is plotted in Fig. 5b. Every bar refers to α achieved by the metafoundation listed on the x-axis, while a single bar refers to the correspondent ground motion in the legend. This plot confirms the improved performance that can be achieved by staggering the columns at the second level of the foundation frame (configuration L2s): as a matter of fact, L2s shows the lowest values of α for most of the accelerograms. The average RMS ratio is α =

1.05, 0.99, 0.79 for L1, L2a and L2s respectively. Therefore, L2s can reduce the hydrodynamic base pressure of about 20%.

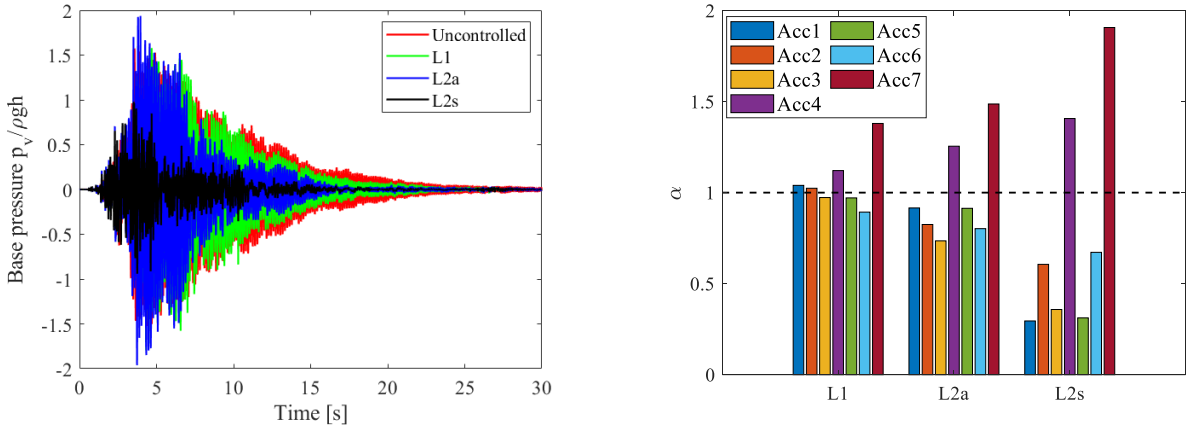

(a) (b)

Fig. 5 – Time history analysis for the accelerogram Acc5: (a) history of base pressure; (b) index α.

Another important use of time history is to validate the assumption of linearly elastic symmetric behaviour of the wire ropes, see Section 2. To this end, we verified the maximum displacement of the resonators and compare it with the limit of elastic behaviour [23]. Fig.6a shows an example of resonators displacement history, while displacement maximum absolute values are plotted in Fig.6b for all the considered foundations. It can be observed that the maximum displacement is always less than 20mm: in that range, the aforementioned assumption is valid according to the tension-compression load-deflection curve given in the catalogue.

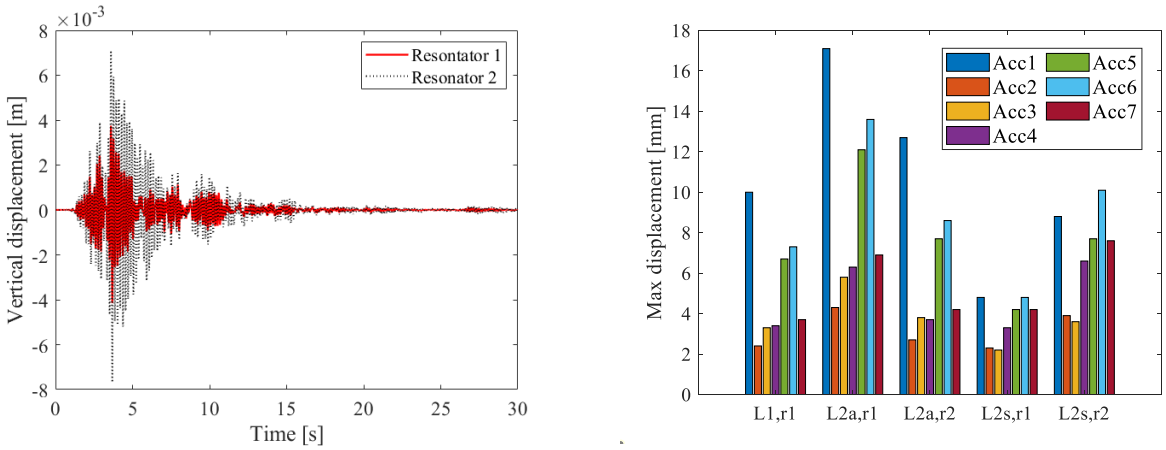

(a) (b)

Fig. 6 – Resonators displacements: (a) history of displacements induced by Acc5; (b) bar plot of the maximum resonator displacement (‘r1’=resonator 1, ‘r2’=resonator 2).

5 Soil-structure interaction

To investigate the influence of soil-structure interaction (SSI) on seismic mitigation performance of periodic foundations, finite element method is employed. Two-dimensional (2D) finite element models (FEMs) of the controlled superstructure with optimal periodic foundation L1 and L2s with SSI included were established, respectively, as well as the uncontrolled superstructure. Then, time history analysis of OBE accelerograms are

done and performance index of breathing pressure and total pressure are employed to indicate influence of SSI of different soil types. For simplicity, SSI on soil type A and C are investigated.

5.1 FE modeling

Illustrations of the FEM of the controlled superstructure with L2s on a soil layer are shown in Fig.7a. The whole system is assumed to behave linearly. The contact between the periodic foundation and the soil is simplified as tie which means no slippage or gap during the calculation.

The superstructure and the outer frame of metafoundation were simulated by beam elements, whereas the inner resonator was modeled using a rigid mass and spring and dashpot elements. The soil was modeled using CPE4R element (a 4-node bilinear plane strain quadrilateral, reduced integration, hourglass control). Rayleigh damping were adopted for the outer frame part and soil part. Corresponding coefficients were calculated based on the first and second frequency of each part, respectively. Damping elements were used to simulate the damping of inner resonators.

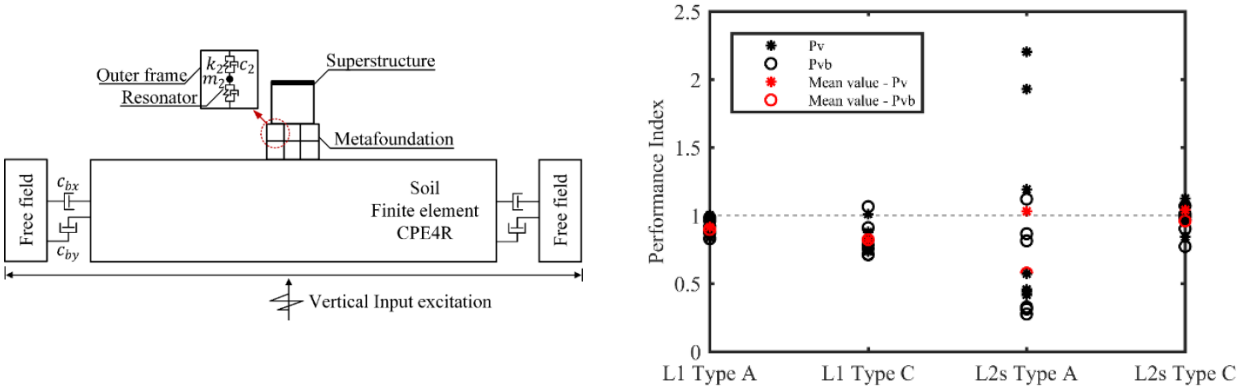

(a) (b)

Fig. 7 – Soil structure interaction: (a) FE model; (b) metafoundation performances on different soils.

The element size in the direction of wave propagation is a key aspect to properly simulate wave propagation. To simulate a vertically propagating shear wave, the height of the element h_{ele} could be taken as $(1/5 - 1/8)v_s/f_{max}$, in which v_s is the shear velocity of the soil layer and f_{max} is the highest wave frequency considered [24]. Similarly, in the case of a primary wave transmitted vertically, the height of the element h_{ele} is taken as $(1/5 - 1/8)v_p/f_{max}$, in which v_p is the primary velocity of the soil layer. The height of the element for both type-A and type-C soil is taken as 0.5 meter.

To properly simulate the horizontally infinite space by using a model with finite size, quite boundary conditions should be applied at boundaries of the soil field to absorb wave reflection. Quite boundary conditions like viscous absorbing boundary, infinite elements and perfectly matched layers have been used in related research [25-27]. Free-field boundaries are employed in this paper. The free-field boundary consists of soil columns to simulate the behavior of the free field and the soil column is connected to each side of the main field by dashpots. As shown in Fig.7a, the lateral boundaries of the main grid are coupled to the free-field grid by viscous dashpots to simulate quiet boundary. The coefficient of dashpot c_x and c_y are given as [24]

$$c_x = \rho v_p \Delta S_y \tag{12}$$

$$c_y = \rho v_s \Delta S_y \tag{13}$$

where ρ is the mass density; v_p and v_s are the primary and shear wave velocities, and ΔS_y is the mean vertical size at boundary grid point. The bottom boundary is considered as a rigid base and a time-history of an accelerogram is applied at base grid points.

5.2 Influence of SSI

Performance indexes based on both the total hydrodynamic base pressure p_v and the breathing mode induced pressure $p_{vb}(t)$ are employed to evaluate the mitigation effect in the time domain, as defined in Eq.(14) and Eq.(15), respectively.

$$PI_v = \sigma_{p_v}^{2,CON}/\sigma_{p_v}^{2,UNC} \tag{14}$$

$$PI_{vb} = \sigma_{p_{vb}}^{2,CON}/\sigma_{p_{vb}}^{2,UNC} \tag{15}$$

Comparisons of seismic mitigation effect of PF L1 and L2s on different types of soils are presented in Fig.7b. For PF L1, a 9% attenuation in average of the total hydrodynamic pressure is achieved on soil type A, while a 18% attenuation in average is obtained on soil type C. Compared with result without SSI, in which the controlled superstructure is slightly amplified as shown in Fig.6b, the performance of L1 is improved due to SSI on both soil type. The mitigation effect on the breathing mode-induced hydrodynamic pressure is similar to that on the total pressure.

Compared with PF L1, the performance of L2s deteriorates due to SSI. As shown in Section 4, when SSI is not included, an average reduction of 22.7% on total pressure for OBE signals is achieved. However, as shown in Fig.7b, for both soil type A and C, the total pressure is averagely amplified, less than 5%. Moreover, the performance of L2s depends on soil type. On soil type A, L2s is effective on mitigate the breathing mode-induced pressure and a 42% reduction in average is achieved. The mitigation effects vary obviously according to different accelerograms. However, on soil type C, the mitigation effects of different accelerograms are closer and, in average, only a slight mitigation effect is achieved.

6 Conclusions

In this paper, we presented feasible metafoundation configurations to protect a slender storage tank against the vertical component of ground shaking. They are distinguished by the number of layers and by the arrangement of columns; in particular, we proposed an unconventional staggered columns frame which, taking advantage of the flexural stiffness of slabs, improves the attenuation capacity of the system. The three systems were optimized and their performances were evaluated through time history analysis. Results lead to the conclusion that the proposed systems are able to attenuate the superstructure response and, therefore, that a metafoundation can be designed for vertical seismic isolation purposes. Moreover, we investigated the influence of SSI on mitigation performance. Results reveal that considering the effects of SSI results in an improved performance of the foundation L1, whereas the attenuation capacity of L2s deteriorates. However, L2s can effectively mitigate the breathing mode induced hydrodynamic pressure on soil type A. Therefore, the influence of SSI deserves deeper investigation and an optimization procedure able to consider this phenomenon should be developed.

7. References

[1] Liu Z, Zhang X, Mao Y, Zhu YY, Yang Z, Chan CT, Sheng P (2000): Locally resonant sonic materials. Science, 289 (5485), 1734-1736.

[2] Jia G, Shi Z (2010): A new seismic isolation system and its feasibility study. *Earthquake Engineering and Engineering Vibration*, **9**(1), 75-82.

[3] Shi Z, Huang J (2013): Feasibility of reducing three-dimensional wave energy by introducing periodic foundations. *Soil Dynamics and Earthquake Engineering*, **50**, 204-212.

[4] Cheng Z, Z Shi (2013): Novel composite periodic structures with attenuation zones. *Engineering Structures*, **56**, 1271-1282.

[5] Yan Y, Laskar A, Cheng Z, Menq F, Tang Y, Mo YL, Shi Z (2014): Seismic isolation of two dimensional periodic foundations. *Journal of Applied Physics*, **116**(4), 044908.

[6] Yan Y, Cheng Z, Menq F, Mo YL, Tang Y, Shi Z (2015): Three dimensional periodic foundations for base seismic isolation. *Smart Materials and Structures*, **24**(7), 075006.

[7] Huang J, Shi Z, Huang W, Chen X, Zhang Z (2017): A periodic foundation with rotational oscillators for extremely low-frequency seismic isolation: analysis and experimental verification. *Smart Materials and Structures*, **26**(3) 035061.

[8] Cheng ZB, Shi ZF (2018): Composite periodic foundation and its application for seismic isolation. *Earthquake Engineering & Structural Dynamics*, **47**(4), 925-944.

[9] Casablanca O, Ventura G, Garescì F, Azzerboni B, Chiaia B, Chiappini M, Finocchio G (2018): Seismic isolation of buildings using composite foundations based on metamaterials. *Journal of Applied Physics*, **123**(17), 174903.

[10] Witarto W, Wang SJ, Yang CY, Wang j, Mo YL, Chang KC, Tang Y (2019): Three-dimensional periodic materials as seismic base isolator for nuclear infrastructure. *AIP Advances*, **9**(4), 045014.

[11] Liu X, Wang Y, Chen Y (2019): Attenuation Zones of Two-Dimensional Periodic Foundations Including the Effect of Vertical Loads. *Applied Sciences*, **9**(5), 993.

[12] La Salandra V, Wenzel M, Bursi OS, Carta G, Movchan AB (2017): Conception of a 3D metamaterial-based foundation for static and seismic protection of fuel storage tanks. *Frontiers in Materials*, **4**, 30.

[13] Wenzel M, Basone F, Bursi OS (2018): Novel Metamaterial-Based Foundation Concept Applied to a Coupled Tank-Pipeline System. *ASME 2018 Pressure Vessels and Piping Conference,* Prague, Czech Republic.

[14] Basone F, Wenzel M, Bursi OS, Fossetti M (2019): Finite locally resonant Metafoundations for the seismic protection of fuel storage tanks. *Earthquake Engineering & Structural Dynamics*, **48**(2), 232-252.

[15] Sun F, Xiao L, Bursi OS (2019): Optimal design and novel configuration of a locally resonant periodic foundation (LRPF) for seismic protection of fuel storage tanks. *Engineering Structures*, **189**, 147-156.

[16] Haroun MA, Tayel MA (1985): Response of tanks to vertical seismic excitations. *Earthquake engineering & structural dynamics*, **13**(5), 583-595.

[17] Lindholm US, Kana DD, Abramson HN (1962): Breathing vibrations of a circular cylindrical shell with an internal liquid. *Journal of the Aerospace Sciences*, **29**(9), 1052-1059.

[18] Alessandri S, Giannini R, Paolacci F, Malena M (2015): Seismic retrofitting of an HV circuit breaker using base isolation with wire ropes. Part 1: Preliminary tests and analyses. *Engineering Structures*, **98**, 251-262.

[19] Alessandri S, Giannini R, Paolacci F, Amoretti M, Freddo A (2015): Seismic retrofitting of an HV circuit breaker using base isolation with wire ropes. Part 2: Shaking-table test validation. *Engineering Structures*, **98**, 263-274.

[20] CS.LL.PP. DM 17 Gennaio (2018): Norme tecniche per le costruzioni. Gazzetta Ufficiale della 43 Repubblica Italiana. *Building Code*, in Italian.

[21] Veletsos AS, Tang Y (1986): Dynamics of vertically excited liquid storage tanks. *Journal of Structural Engineering*, **112** (6), 1228-1246.

[22] Eurocode 8 - Design of structures for earthquake resistance- Part 4: Silos, tanks andpipelines. *Design Code*. London, UK: CEN, 2015

[23] Wire Rope Isolators. https://www.enidine.com/en-US/Products/WireRopeIsolator/. Produced by ENIDINE.

[24] Luo C, Yang X, Zhan C, Jin X, Ding Z (2016): Nonlinear 3D finite element analysis of soil–pile–structure interaction system subjected to horizontal earthquake excitation. *Soil Dynamics and Earthquake Engineering*, **84**, 145-156.

[25] Van Nguyen Q, Fatahi B, Hokmabadi AS (2017): Influence of size and load-bearing mechanism of piles on seismic performance of buildings considering soil–pile–structure interaction. *International Journal of Geomechanics*, **17** (7), 04017007.

[26] Zhang C, Pan J, and Wang J (2009): Influence of seismic input mechanisms and radiation damping on arch dam response. *Soil Dynamics and Earthquake Engineering*, **29** (9), 1282-1293.

[27] Shih JY, Thompson DJ, Zervos A, (2016) The effect of boundary conditions, model size and damping models in the finite element modelling of a moving load on a track/ground system. *Soil Dynamics and Earthquake Engineering*, **89**, 12-27.

